



**HAL**  
open science

## **Wnt, glucocorticoid and cellular prion protein cooperate to drive a mesenchymal phenotype with poor prognosis in colon cancer**

Sophie Mouillet-Richard, Angélique Gougelet, Bruno Passet, Camille Brochard, Delphine Le Corre, Caterina Luana Pitasi, Camille Joubel, Marine Sroussi, Claire Gallois, Julien Lavergne, et al.

### ► To cite this version:

Sophie Mouillet-Richard, Angélique Gougelet, Bruno Passet, Camille Brochard, Delphine Le Corre, et al.. Wnt, glucocorticoid and cellular prion protein cooperate to drive a mesenchymal phenotype with poor prognosis in colon cancer. *Journal of Translational Medicine*, 2024, 22, 10.1186/s12967-024-05164-0 . hal-04538247

**HAL Id: hal-04538247**

**<https://hal.science/hal-04538247>**

Submitted on 9 Apr 2024

**HAL** is a multi-disciplinary open access archive for the deposit and dissemination of scientific research documents, whether they are published or not. The documents may come from teaching and research institutions in France or abroad, or from public or private research centers.


L'archive ouverte pluridisciplinaire **HAL**, est destinée au dépôt et à la diffusion de documents scientifiques de niveau recherche, publiés ou non, émanant des établissements d'enseignement et de recherche français ou étrangers, des laboratoires publics ou privés.

RESEARCH

Open Access



# Wnt, glucocorticoid and cellular prion protein cooperate to drive a mesenchymal phenotype with poor prognosis in colon cancer

Sophie Mouillet-Richard<sup>1,5\*</sup> , Angélique Gougelet<sup>1†</sup>, Bruno Passet<sup>2†</sup>, Camille Brochard<sup>1,3†</sup>, Delphine Le Corre<sup>1,5</sup>, Caterina Luana Pitasi<sup>4,5</sup>, Camille Joubel<sup>1,5</sup>, Marine Sroussi<sup>1,5</sup>, Claire Gallois<sup>1,5,6</sup>, Julien Lavergne<sup>1,7</sup>, Johan Castille<sup>2</sup>, Marthe Vilotte<sup>2</sup>, Nathalie Daniel-Carlier<sup>2</sup>, Camilla Pilati<sup>1,5</sup>, Aurélien de Reyniès<sup>1,5</sup>, Fatima Djouadi<sup>1,5</sup>, Sabine Colnot<sup>1,5</sup>, Thierry André<sup>8</sup>, Julien Taieb<sup>1,5,6</sup>, Jean-Luc Vilotte<sup>2</sup>, Béatrice Romagnolo<sup>4,5</sup> and Pierre Laurent-Puig<sup>1,5,9\*</sup>

## Abstract

**Background** The mesenchymal subtype of colorectal cancer (CRC), associated with poor prognosis, is characterized by abundant expression of the cellular prion protein PrP<sup>C</sup>, which represents a candidate therapeutic target. How PrP<sup>C</sup> is induced in CRC remains elusive. This study aims to elucidate the signaling pathways governing PrP<sup>C</sup> expression and to shed light on the gene regulatory networks linked to PrP<sup>C</sup>.

**Methods** We performed *in silico* analyses on diverse datasets of *in vitro*, *ex vivo* and *in vivo* models of mouse CRC and patient cohorts. We mined ChIPseq studies and performed promoter analysis. CRC cell lines were manipulated through genetic and pharmacological approaches. We created mice combining conditional inactivation of *Apc* in intestinal epithelial cells and overexpression of the human prion protein gene *PRNP*. Bio-informatic analyses were carried out in two randomized control trials totalizing over 3000 CRC patients.

**Results** *In silico* analyses combined with cell-based assays identified the Wnt- $\beta$ -catenin and glucocorticoid pathways as upstream regulators of *PRNP* expression, with subtle differences between mouse and human. We uncover multiple feedback loops between PrP<sup>C</sup> and these two pathways, which translate into an aggravation of CRC pathogenesis in mouse. In stage III CRC patients, the signature defined by *PRNP-CTNNB1-NR3C1*, encoding PrP<sup>C</sup>,  $\beta$ -catenin and the glucocorticoid receptor respectively, is overrepresented in the poor-prognosis, mesenchymal subtype and associates with reduced time to recurrence.

**Conclusions** An unleashed PrP<sup>C</sup>-dependent vicious circle is pathognomonic of poor prognosis, mesenchymal CRC. Patients from this aggressive subtype of CRC may benefit from therapies targeting the *PRNP-CTNNB1-NR3C1* axis.

**Keywords** Colon cancer, Prion protein, Wnt- $\beta$ -catenin, Glucocorticoid receptor, Molecular classification

<sup>†</sup>Angélique Gougelet, Bruno Passet, Camille Brochard contributed equally to this work.

\*Correspondence:

Sophie Mouillet-Richard  
[sophie.mouillet-richard@parisdescartes.fr](mailto:sophie.mouillet-richard@parisdescartes.fr)  
Pierre Laurent-Puig  
[pierre.laurent-puig@parisdescartes.fr](mailto:pierre.laurent-puig@parisdescartes.fr)

Full list of author information is available at the end of the article



© The Author(s) 2024. **Open Access** This article is licensed under a Creative Commons Attribution 4.0 International License, which permits use, sharing, adaptation, distribution and reproduction in any medium or format, as long as you give appropriate credit to the original author(s) and the source, provide a link to the Creative Commons licence, and indicate if changes were made. The images or other third party material in this article are included in the article's Creative Commons licence, unless indicated otherwise in a credit line to the material. If material is not included in the article's Creative Commons licence and your intended use is not permitted by statutory regulation or exceeds the permitted use, you will need to obtain permission directly from the copyright holder. To view a copy of this licence, visit <http://creativecommons.org/licenses/by/4.0/>. The Creative Commons Public Domain Dedication waiver (<http://creativecommons.org/publicdomain/zero/1.0/>) applies to the data made available in this article, unless otherwise stated in a credit line to the data.

## Background

With over 900,000 deaths in 2020, colorectal cancer (CRC) remains the third most frequent cancer and the second cause of cancer-related deaths worldwide [1]. Despite tremendous progress in screening, diagnosis and therapy, the 5-years relative survival rate remains 65% (all disease stages), and even drops below 15% when patients are diagnosed at the metastatic stage (stage IV). Achieving a better understanding of the complex molecular mechanisms that orchestrate CRC pathogenesis still remains among the greatest challenges to improve therapeutic strategies.

Ever since the seminal identification of *APC* gene mutations associated with familial adenomatous polyposis over 30 years ago [2], the Wnt- $\beta$ -catenin has remained the top-most scrutinized signaling pathway in CRC [3]. Around 90% of CRC cases have somatic mutations in the *APC* gene or other components of the Wnt pathway [3]. Although disturbed Wnt signaling is a constant feature in CRC, our knowledge of the co-regulatory pathways that cooperate with Wnt- $\beta$ -catenin to promote CRC progression or that dictate specific transcriptional programs according to CRC molecular subtypes is far from complete. Indeed, the consensus molecular classification of CRC enables to divide tumors into one major or a combination of consensus molecular subtypes (CMS) based on bulk transcriptome profiling [4, 5]. Because *APC* mutations are prevalent in all CMS, although less frequent in the CMS1 subtype that corresponds to hypermutated and microsatellite unstable tumors [4], it can be surmised that CMS-specific signaling cascades orientate the Wnt response. In the CMS4 subtype that is associated with dismal prognosis, two pathways, namely TGF $\beta$  [6] and YAP/TAZ [7], have gathered special interest. These pathways are well known to crosstalk with Wnt- $\beta$ -catenin signaling [8], and, therefore, are good candidates for influencing the Wnt- $\beta$ -catenin output. Recently, we documented that the cellular prion protein PrP<sup>C</sup>, encoded by the *PRNP* gene, is an upstream regulator of these two major pathways in CMS4 CRC [9], and that its targeting is a promising approach to treat CMS4 patients [10]. Long confined to the field of neurodegenerative diseases, PrP<sup>C</sup> is now attracting a great deal of interest in cancer research [11]. Its location at the cell membrane [12], coupled to its capacity to instruct downstream cell signaling events [13] make it an ideal candidate for fine-tuning the cellular response to environmental signals. One unanswered question relates to the induction of *PRNP* expression along CRC initiation and progression. By integrating in silico analyses on mouse and human datasets with cell-based experiments, we provide evidence that *PRNP* expression is jointly controlled by the Wnt and glucocorticoid signaling pathways. Using mice that combine

*Apc* inactivation in intestinal epithelial cells and *PRNP* overexpression, we uncover a positive Wnt-PrP<sup>C</sup> feedback loop that unleashes a vicious circle. Analyses carried out in several mouse models of  $\beta$ -catenin-driven liver cancer corroborated the occurrence of a Wnt-PrP<sup>C</sup> axis. Our data further point to species differences in the regulation of *PRNP* expression, with glucocorticoid signaling playing a critical role in human as compared to mouse. Finally, we show in two randomized clinical trials (RCT) of stage III CRC, altogether encompassing over 3000 patients, that the PrP<sup>C</sup>-dependent axis is pathognomonic of the CMS4 subtype and is associated with dismal prognosis.

## Methods

### Gene expression analyses

The following datasets were retrieved from public sources: GSE200908 [14], GSE208372 [15], GSE167008 [16], GSE20916 [17], GSE8671 [18], GSE4183 [19], GSE39852 [20], GSE11406 [21], PRJEB44400 [22]. Due to missing values, some analyses could not be performed with the GSE20916 dataset. Kinetic RNAseq data from sorted *Apc*<sup>Δhep</sup> hepatocytes are deposited on GEO with accession number GSE210482 [23].

### Patients cohorts and analyses

The IDEA-France cohort is composed of 1248 patients having signed informed consent within a phase III randomized trial comparing 3 months to 6 months of mFOLFOX6 (infusional fluorouracil, leucovorin, and oxaliplatin) or CAPOX (capecitabine, oxaliplatin) after curative resection of stage III CC [24], and for which we obtained RNAseq on punch biopsies, as described in [25].

The PETACC8 cohort is composed of 1733 patients having signed informed consent within a phase III randomized trial comparing FOLFOX4 (infusional fluorouracil, leucovorin, and oxaliplatin) to FOLFOX4 + cetuximab in 2550 patients after curative resection of stage III CC [26], and for which we obtained RNAseq on macrodissected formalin-fixed, paraffin-embedded (FFPE) tissue sections, as described in [25].

The demographics of the IDEA-France and the PETACC8 cohorts are summarized in Additional file 1: Tables S1 and S2, respectively.

3'RNAseq and bioinformatics analyses are detailed in Additional file 1.

For survival analyses, the optimal cutpoint value was determined to predict time to recurrence (TTR), using the `surv_cutpoint` function from R package `survminer`. TTR analyses were performed using the `coxph` function of the survival R package. All analyses were carried out using R studio (version 4.2.2).

### Statistical analysis

RNAseq datasets (GSE200908, GSE208372, GSE167008, PRJEB44400) were analyzed using the DESeq2 package version 1.38.3. All analyses were performed with R studio 4.2.2. All statistical analyses were performed in R studio (version 4.2.2) using the `stat_compare_means` function from the `ggpubr` package. Correlation analyses were performed in R studio (version 4.2.2) using the `stat_cor` function from the `ggpubr` package. The results from experimental data in cell lines are reported as the means  $\pm$  standard errors of the means (s.e.m.) with graphs generated using GraphPad PRISM version 9.4.1. Analyses involving two groups were carried out using the Shapiro test followed by Student's t test or Mann–Whitney rank-sum test according to normality. Results from RT-qPCR in mouse tissue and RNA analysis in public datasets or patient cohorts are expressed as median and interquartile range with graphs generated with `ggplot2` in R studio. Statistical analysis was performed using the Mann–Whitney rank-sum test for two groups or one-way ANOVA followed by Wilcoxon rank-sum tests with Holm's correction for multiple comparisons for  $> 2$  groups.

Additional materials and methods are described in Additional file 1.

## Results

### PRNP is a target of Wnt- $\beta$ -catenin signaling in various models of $\beta$ -catenin-activated intestinal tumors

A still unresolved question regarding the overexpression of the cellular prion protein in colon cancer relates to the molecular pathways involved. By interrogating public datasets, we found that Apc inactivation in several mouse experimental paradigms, i.e. in the murine MC38 colon cancer cell line (GSE200908 [14]), mouse colonic tumor organoids (GSE208372 [15]), or mouse intestinal tumors (GSE167008 [16]), was systematically associated with *Prnp* gene upregulation (Fig. 1A–C). Assuming that *PRNP* might be a target of the canonical Wnt- $\beta$ -catenin pathway, we subsequently mined ChIPseq datasets for  $\beta$ -catenin binding. As shown in Fig. 1D, we found that the *PRNP* promoter is occupied by  $\beta$ -catenin and harbors the active H3K4me3 mark (H3 histone tri-methylated on Lysine 4) in SW480 and DLD1 colon cancer cells in the GSE156083 dataset [27]. Likewise, searching the ENCODE database, we found that the *PRNP* promoter is bound by the *TCF7L2* gene-encoded TCF4 transcription factor, the main  $\beta$ -catenin co-factor in colon and liver, as well as H3K27ac (H3 histone acetylated on Lysine 27) and H3K4me3, which both mark active chromatin, in HCT116 colon cancer cells (Fig. 1E). We further identified one TCF4 binding site in the promoter of *PRNP* by analyzing predicted transcription factor binding sites

using the JASPAR database [28] (Fig. 1F). In agreement with the above data, *PRNP* expression was significantly reduced in  $\beta$ -catenin-silenced MDST8 colon cancer cells (Fig. 1G, H). Altogether these data show that  $\beta$ -catenin/TCF4 bind Wnt-responsive element (WRE)-encompassing enhancers specifically active in *PRNP* in human  $\beta$ -catenin activated tumor cells.

### PRNP is a target of the glucocorticoid receptor in CRC cells

Turning to CRC patients, we analyzed the expression profile of *PRNP* along disease progression from normal to adenoma to carcinoma. In three distinct datasets GSE8671 [18], GSE20916 [17] and GSE4183 [19], we recurrently found decreased expression of *PRNP* transcripts in adenoma versus normal tissue (Fig. 2A–C), contrasting with the increase in the expression of several Wnt target genes including *AXIN2* [18]. On another hand, colon cancer tissue exhibited higher amounts of *PRNP* as compared to both adenoma and normal tissue (Fig. 2B, C), confirming the previous report by de Wit et al. that PrP<sup>C</sup> is induced along the adenoma-carcinoma sequence [29]. It is well established that the recruitment of  $\beta$ -catenin to target genes is not always sufficient to induce transcription and that  $\beta$ -catenin-dependent transcriptional regulation is highly context-specific and often involves co-factors [30]. Because the Wnt pathway is switched on in adenomas but is not accompanied by an increase in *PRNP* mRNAs, in contrast to our observations in mouse models, we thus surmised that  $\beta$ -catenin may cooperate with (an)other regulatory factor(s) to promote *PRNP* transcription in human cells. To identify potential candidates, we selected the transcription factors (TF) that fulfil the following criteria: (1) binding to the *PRNP* gene in the ENCODE database and (2) featuring in the HIPPIE (Human Integrated Protein–Protein Interaction rEference, [31]) database of  $\beta$ -catenin interactors. We further filtered the list of 11 candidates to keep TF whose expression is significantly correlated to that of *PRNP* in the two patient datasets GSE4183 and GSE39852 [20] (Fig. 2D). *NR3C1*, which encodes the glucocorticoid receptor, GR, was more strongly correlated with *PRNP* in the GSE39852 dataset than was *ETS1* ( $R=0.45$  versus  $R=0.32$ ) and was selected for further analysis (Fig. 2E). Using the JASPAR database, we identified a consensus palindromic binding motif for NR3C1 in the *PRNP* promoter (Fig. 2F). Of note, this sequence is not conserved in the mouse *Prnp* promoter sequence (Additional file 1: Fig. S1A), although another GR responsive element (GRE) is found further upstream, according to JASPAR analysis (Additional file 1: Fig. S1B), in contrast to the WRE that is conserved from human to mouse (Additional file 1: Fig. S1A). The expression profile of *NR3C1* is highly compatible with a GR-dependent

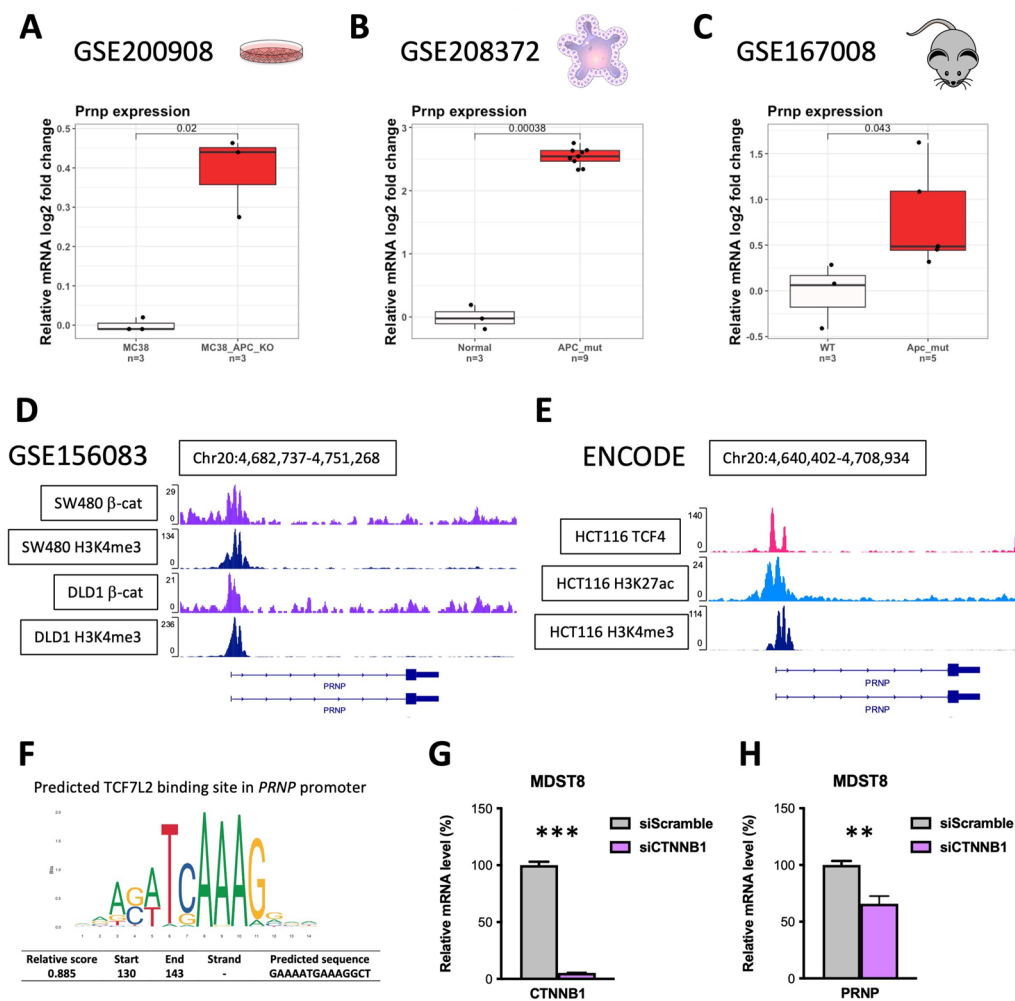


**Fig. 1** The *PRNP* gene is a target of Wnt- $\beta$ -catenin signaling in colon cancer models. **A–C** Analysis of the GSE200908 (**A**) GSE208372 (**B**) and GSE167008 (**C**) datasets reveals increased *Prnp* expression in cellular, organoid and in vivo mouse models of *Apc* inactivation. **D** Analysis of the GSE156083 ChIPseq dataset reveals enrichment of  $\beta$ -catenin and the H3K4me3 active histone mark at the promoter of the *PRNP* gene in SW480 and DLD-1 human colon cancer cell lines. **E** Analysis from the ENCODE database reveals binding of the TCF7L2-encoded TCF4 factor, together with the H3K27ac and H3K4me3 active histone marks at the promoter of the *PRNP* gene in the HCT116 human colon cancer cell line. **F** Predicted TCF7L2 binding site within the human *PRNP* gene promoter. **G, H** Relative mRNA levels of *CTNNB1* (**G**) and *PRNP* (**H**) in *CTNNB1*-silenced versus control MDST8 cells, as determined in qPCR analysis. Results are expressed as means of  $n=2$  independent triplicates of cell preparations  $\pm$  s.e.m. (\*\* $p < 0.01$ , \*\*\* $p < 0.001$ , Student's *t*-test)

regulation of *PRNP* gene expression since it is most abundantly expressed in the CMS4 subtype of CRC (Fig. 2G), it globally follows the pattern of *PRNP* expression along the normal to adenoma to adenocarcinoma sequence in patients (Fig. 2H–J), and *NR3C1* and *PRNP* levels are significantly correlated in various datasets (Fig. 2K–M).

Because the expression of *NR3C1* mRNA cannot be considered as a readout of GR activation, we reasoned that if *PRNP* is indeed a GR target, then it should be co-expressed with well-established GR-regulated genes. Indeed, *TSC22D3*, also known as Glucocorticoid-Inducible Leucine Zipper (*GILZ*), features among the top-50

*PRNP* positively correlated genes in the GSE4183 dataset (Fig. 3A). As observed with *NR3C1*, *TSC22D3* transcripts are reduced in adenoma versus normal tissue but further induced at the adenoma-to-carcinoma progression (Fig. 3B, C); they strongly correlate with *PRNP* levels, including in the large GSE39582 dataset (Fig. 3D–F) and are enriched in CMS4 CRC (Fig. 3G). We then assessed whether *PRNP* transcription is induced upon GR activation. In the GSE11406 dataset [21], *Prnp* levels were induced in oligodendrocyte progenitor cells (OPC) after exposure to Dexamethasone (Dex) in a time-dependent manner (Fig. 3H). Likewise, we found

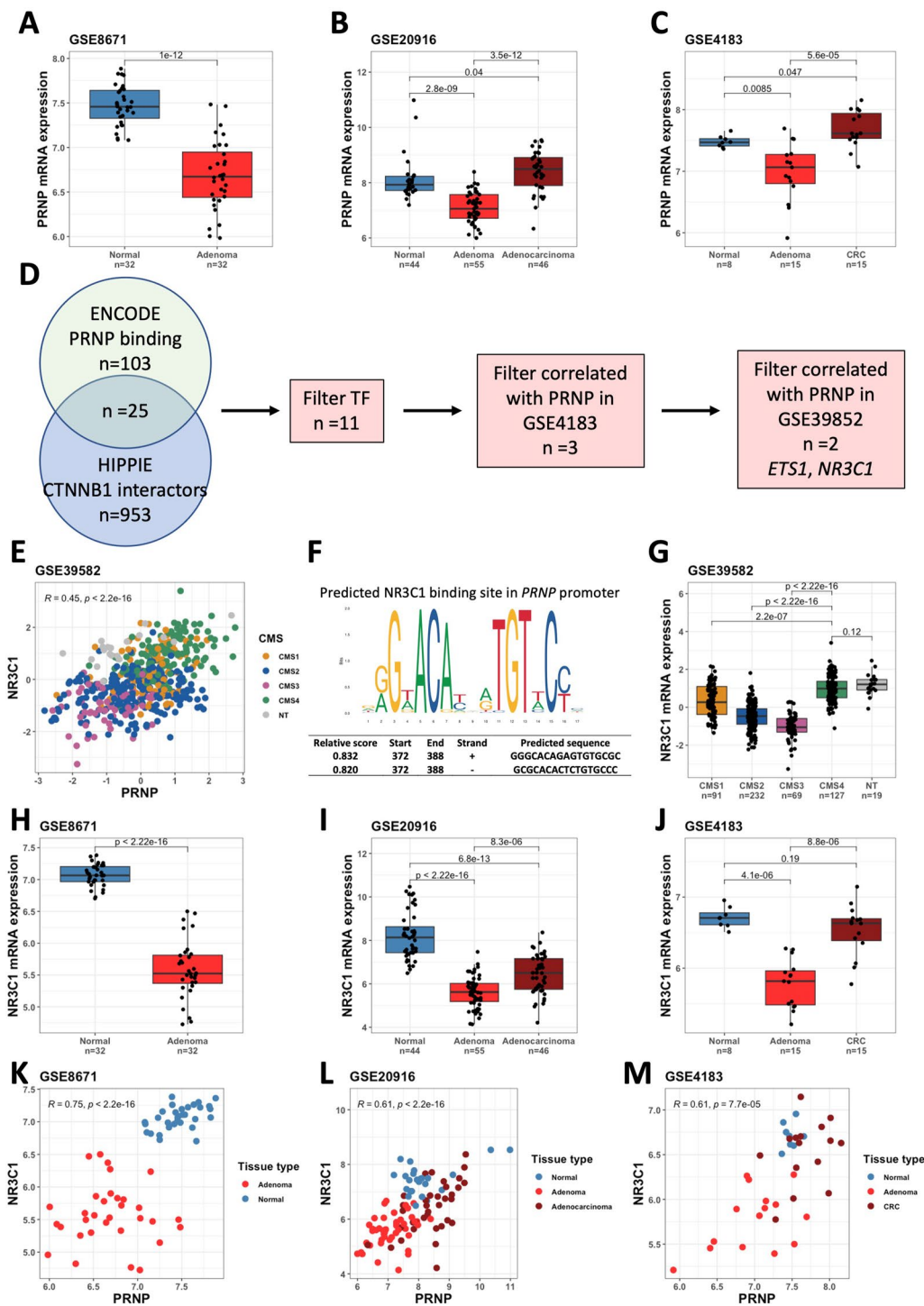


**Fig. 2** The GR encoded by the *NR3C1* gene is predicted to regulate *PRNP* gene expression in human CRC. **A–C** Analysis of the GSE8671 (**A**) GSE20916 (**B**) and GSE4183 (**C**) datasets reveals decreased *PRNP* expression across the normal to adenoma sequence, followed by an increase from the adenoma to carcinoma sequence in human CRC. **D** Schematic representation of the selection of *ETS1* and *NR3C1* as candidate transcription factors regulating the expression of *PRNP* in human CRC. **E** Scatter plot showing the correlation between *PRNP* and *NR3C1* mRNA levels in the GSE39582 dataset of human CRC. **F** Predicted NR3C1 binding sites within the human *PRNP* gene promoter. **G** Relative *NR3C1* mRNA levels according to the CMS classification in the GSE39582 dataset of human CRC. NT = non tumor. **H–J** Analysis of the GSE8671 (**H**) GSE20916 (**I**) and GSE4183 (**J**) datasets reveals decreased *NR3C1* expression across the normal to adenoma sequence, followed by an increase from the adenoma to carcinoma sequence in human CRC. **K–M** Scatter plots showing the correlation between *PRNP* and *NR3C1* mRNA levels in GSE8671 (**K**) GSE20916 (**L**) and GSE4183 (**M**) datasets

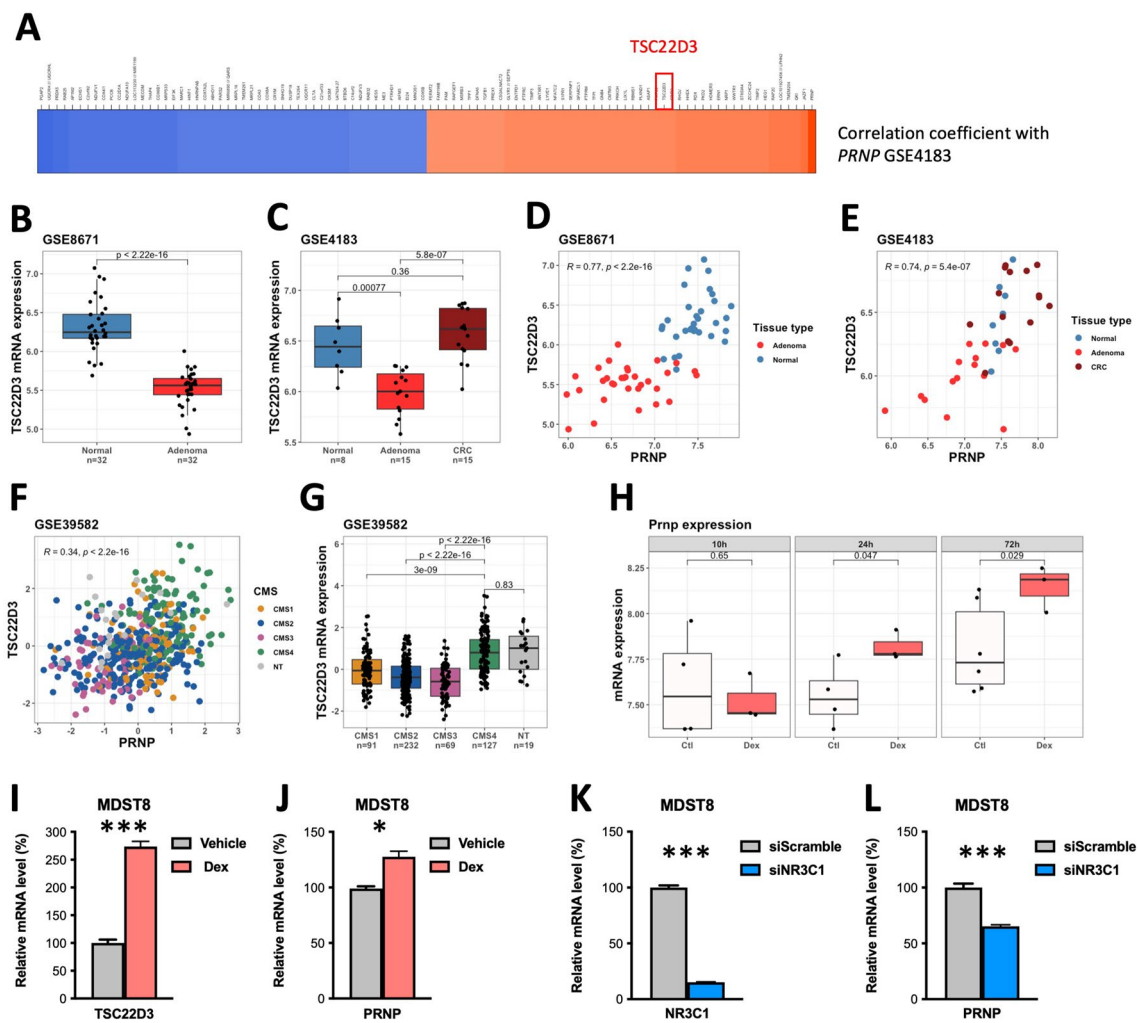


**Fig. 3** *PRNP* gene expression is regulated by the GR in human CRC. **A** Heatmap showing the top 20 positively (in red) and negatively (in blue) correlated genes to *PRNP* expression in the GSE4183 dataset. Highlighted is the GR target *TSC22D3*. **B, C** Analysis of the GSE8671 (**B**) and GSE4183 (**C**) datasets reveals decreased *TSC22D3* expression across the normal to adenoma sequence, followed by an increase from the adenoma to carcinoma sequence in human CRC. **D, E** Scatter plots showing the correlation between *PRNP* and *TSC22D3* mRNA levels in GSE8671 (**D**) and GSE4183 (**E**) datasets. **F** Scatter plot showing the correlation between *PRNP* and *TSC22D3* mRNA levels in the GSE39582 dataset of human CRC. **G** Relative *TSC22D3* mRNA levels according to the CMS classification in the GSE39582 dataset of human CRC. NT = non tumor. **H** Boxplots showing the time-dependent increase in *Pmp* expression in oligodendrocyte progenitor cells (OPCs) exposed to Dexamethasone (Dex) (GSE11406 dataset). **I, J** Relative mRNA levels of *TSC22D3* (**I**) and *PRNP* (**J**) in MDST8 cells exposed to Dex (1  $\mu$ M, 24 h) versus vehicle (water), as determined in qPCR analysis.  $n=3$  cell preparations per condition. (\*\*\*) $p < 0.001$ , (\*) $p < 0.05$ , Student's t-test). **K, L** Relative mRNA levels of *NR3C1* (**K**) and *PRNP* (**L**) in *NR3C1*-silenced versus control MDST8 cells, as determined in qPCR analysis.  $n=2$  independent triplicates of cell preparations. (\*\*\*) $p < 0.001$ , Student's t-test

increased expression of *PRNP* in the MDST8 CRC cell line upon treatment with Dex (1  $\mu$ M, 24 h), accompanying increased *TSC22D3* expression (Fig. 3I–J). Reciprocally, *PRNP* levels were reduced in *NR3C1*-silenced MDST8 cells (Fig. 3K, L). Combined with our previous report that PrP<sup>C</sup> controls the expression of NR3C1 in CRC cells [9], these data provide evidence for a positive feedback loop linking PrP<sup>C</sup> to the GR and suggest that the GR may cooperate with  $\beta$ -catenin to regulate *PRNP* gene expression in CRC.

### PrP<sup>C</sup> overexpression boosts Wnt signaling in mouse intestine

According to our previous findings and the above data, PrP<sup>C</sup> sustains positive feedback loops with multiple effectors in colon cancer cells: TGF $\beta$ 1 [9], but also the integrin linked kinase (ILK) [32], the amyloid precursor protein (APP)-derived A $\beta$  [10], or the GR (cf above). This prompted us to investigate whether this would also apply to the Wnt pathway. This hypothesis is notably supported by the demonstration by Besnier et al. that PrP<sup>C</sup> interacts

with  $\beta$ -catenin and its cofactor TCF7L2 and upregulates the transcriptional activity of the  $\beta$ -catenin/TCF7L2 complex in SW480 cells [33]. Corroborating this finding, we found that PrP<sup>C</sup> silencing in MDST8 or SW480 colon cancer cells reduced the levels of *AXIN2* mRNA, while its overexpression in LoVo cells was associated to an opposite increase in *AXIN2* transcripts (Additional file 1: Fig. S2). To test our hypothesis, we sought to generate mice combining inducible *Apc* inactivation with PrP<sup>C</sup> overexpression with the idea that a PrP<sup>C</sup>-Wnt positive feedback loop would translate into an increase in Wnt targets in normal tissue of PrP<sup>C</sup> overexpressing mice and sustain a vicious circle amplifying the expression of PrP<sup>C</sup> itself as well as its targets in *Apc*-mutant tumors. Mice containing a floxed mutant allele of the *Apc* gene (*Apc*<sup>fl/+</sup>) [34] as well as tamoxifen-dependent Cre-recombinase under the control of the Villin promoter (*Vill-cre*) [35], i.e. *Vil-CreER*<sup>T2</sup>*Apc*<sup>fl/+</sup> mice [36], were crossed with mice overexpressing the human *PRNP* gene under its own regulatory sequences (through the use of a transgene composed of a large human genomic insert purified from a P1-derived artificial chromosome), in an endogenous mouse *Prnp*-null context (*PRNP*<sup>+/+</sup>*Prnp*<sup>-/-</sup>, hereafter referred to as *PRNP*<sup>+/+</sup>) [37], as outlined in Additional file 1: Fig. S3A. Importantly, the latter so-called tg650 mice have been extensively used in prion studies and were not reported to spontaneously overdevelop tumors compared to wild-type mice (personal communication JLV), indicating that PrP<sup>C</sup> overexpression per se does not initiate tumorigenesis. On another hand, these mice moderately overexpress PrP<sup>C</sup> in the heterozygous state (*PRNP*<sup>+/-</sup>) and overexpress PrP<sup>C</sup> sixfold versus WT in the homozygous state (*PRNP*<sup>+/+</sup>) [37]. They further allow to capture regulatory events impacting *PRNP* expression, contrary to the tga20 mouse model that overexpresses murine *Prnp* (eightfold) in an unregulated fashion [38]. To induce *Apc* loss of function, *VilCreER*<sup>T2</sup>*Apc*<sup>fl/+</sup>-*PRNP*<sup>+/-</sup> and *VilCreER*<sup>T2</sup>*Apc*<sup>fl/+</sup>-*PRNP*<sup>+/+</sup> mice were treated with tamoxifen (see Materials and Methods) and maintained until they showed signs of intestinal illness. Several tamoxifen-untreated *VilCreER*<sup>T2</sup>*Apc*<sup>fl/+</sup>-*PRNP*<sup>+/-</sup> or Cre-negative *Apc*<sup>fl/+</sup>-*PRNP*<sup>+/-</sup> mice remained healthy at comparable time points, confirming that the loss of function

of *Apc* is mandatory to initiate tumorigenesis in this mouse model (data not shown). We then harvested tissue from *VilCreER*<sup>T2</sup>*Apc*<sup>fl/+</sup>-*PRNP*<sup>+/-</sup> and *VilCreER*<sup>T2</sup>*Apc*<sup>fl/+</sup>-*PRNP*<sup>+/+</sup> mice and assessed the expression of several markers of interest through RT-qPCR. As shown in Additional file 1: Fig. S3B, *PRNP* levels were comparable in control (tamoxifen-untreated *VilCreER*<sup>T2</sup>*Apc*<sup>fl/+</sup>-*PRNP*<sup>+/-</sup> or Cre-negative *Apc*<sup>fl/+</sup>-*PRNP*<sup>+/-</sup>) and tamoxifen-treated *VilCreER*<sup>T2</sup>*Apc*<sup>fl/+</sup>-*PRNP*<sup>+/-</sup> normal tissue, indicating that *PRNP* gene expression is insensitive to tamoxifen treatment. Then, we compared the normal tissues of *PRNP*<sup>+/-</sup> and *PRNP*<sup>+/+</sup> mice. Elevated expression of *PRNP* in homozygous mice (Additional file 1: Fig. S4A) was accompanied by increased expression of a set of genes that we previously identified as PrP<sup>C</sup> gene targets in colon cancer cells [10], namely *App*, *Bace1*, *Dkk3*, *Pdgfc* and *Tgfb1* (Additional file 1: Fig. S4B–F), thus validating our model as a robust *PRNP*-overexpressing paradigm. We further recorded increased expression of the canonical Wnt target genes *Axin2*, *Lgr5* and *Ccnd1* in homozygous *PRNP*<sup>+/+</sup> mice versus their heterozygous counterparts (Additional file 1: Fig. S4G–I). As observed for *PRNP*, PrP<sup>C</sup>-dependent target genes (Additional file 1: Fig. S3C–G) and canonical Wnt target genes (Additional file 1: Fig. S3H–J) were not sensitive to tamoxifen treatment per se. As a whole, these data support our hypothesis that PrP<sup>C</sup> boosts Wnt signaling.

#### **PrP<sup>C</sup> overexpression aggravates oncogenic *Apc*-induced colon tumorigenesis**

We went on to examine the impact of PrP<sup>C</sup> overexpression on the same set of genes in intestinal tumors. We first found that *PRNP* mRNA levels were elevated in intestinal tumors versus normal tissue, whatever the genetic status (hetero- or homozygous) of the mice (Fig. 4A). The mean *PRNP* levels measured in the tumors of *PRNP*<sup>+/-</sup> mice however remained inferior to that measured in the normal tissue of *PRNP*<sup>+/+</sup> mice. In the end, the mean *PRNP* mRNA level found in *PRNP*<sup>+/+</sup> tumors reached 3.8 fold that of *PRNP*<sup>+/-</sup> tumors. In agreement with the above findings, we also found that the expression of the PrP<sup>C</sup> target genes *App*, *Bace1*, *Dkk3*, *Pdgfc* and *Tgfb1* were all increased in the tumor versus

(See figure on next page.)

**Fig. 4** PrP<sup>C</sup> sustains a vicious circle in an oncogenic *Apc* mouse model. **A–F** Boxplots showing the mRNA levels of human *PRNP* (**A**), and mouse *App* (**B**), *Bace1* (**C**), *Dkk3* (**D**), *Pdgfc* (**E**) and *Tgfb1* (**F**) in normal or tumor tissue from *VilCreER*<sup>T2</sup>*Apc*<sup>fl/+</sup>-*PRNP*<sup>+/-</sup> (*PRNP*\_het) or *VilCreER*<sup>T2</sup>*Apc*<sup>fl/+</sup>-*PRNP*<sup>+/+</sup> (*PRNP*\_hom) mice as measured through qRT-PCR. **G–N** Scatter plots showing the correlation between the mRNA levels of human *PRNP* and those of mouse *App* (**G**), *Bace1* (**H**), *Dkk3* (**I**), *Pdgfc* (**J**), *Tgfb1* (**K**), *Axin2* (**L**), *Lgr5* (**M**) and *Ccnd1* (**N**) in normal or tumor tissue from *VilCreER*<sup>T2</sup>*Apc*<sup>fl/+</sup>-*PRNP*<sup>+/-</sup> or *VilCreER*<sup>T2</sup>*Apc*<sup>fl/+</sup>-*PRNP*<sup>+/+</sup> mice. **O, P** Boxplots showing the mRNA levels of mouse *Axin2* (**O**) and *Ccnd1* (**P**) in normal or tumor tissue from *VilCreER*<sup>T2</sup>*Apc*<sup>fl/+</sup>-*PRNP*<sup>+/-</sup> (*PRNP*\_het) or *VilCreER*<sup>T2</sup>*Apc*<sup>fl/+</sup>-*PRNP*<sup>+/+</sup> (*PRNP*\_hom) mice as measured through qRT-PCR. Mice experiments were conducted as described in Additional file 1



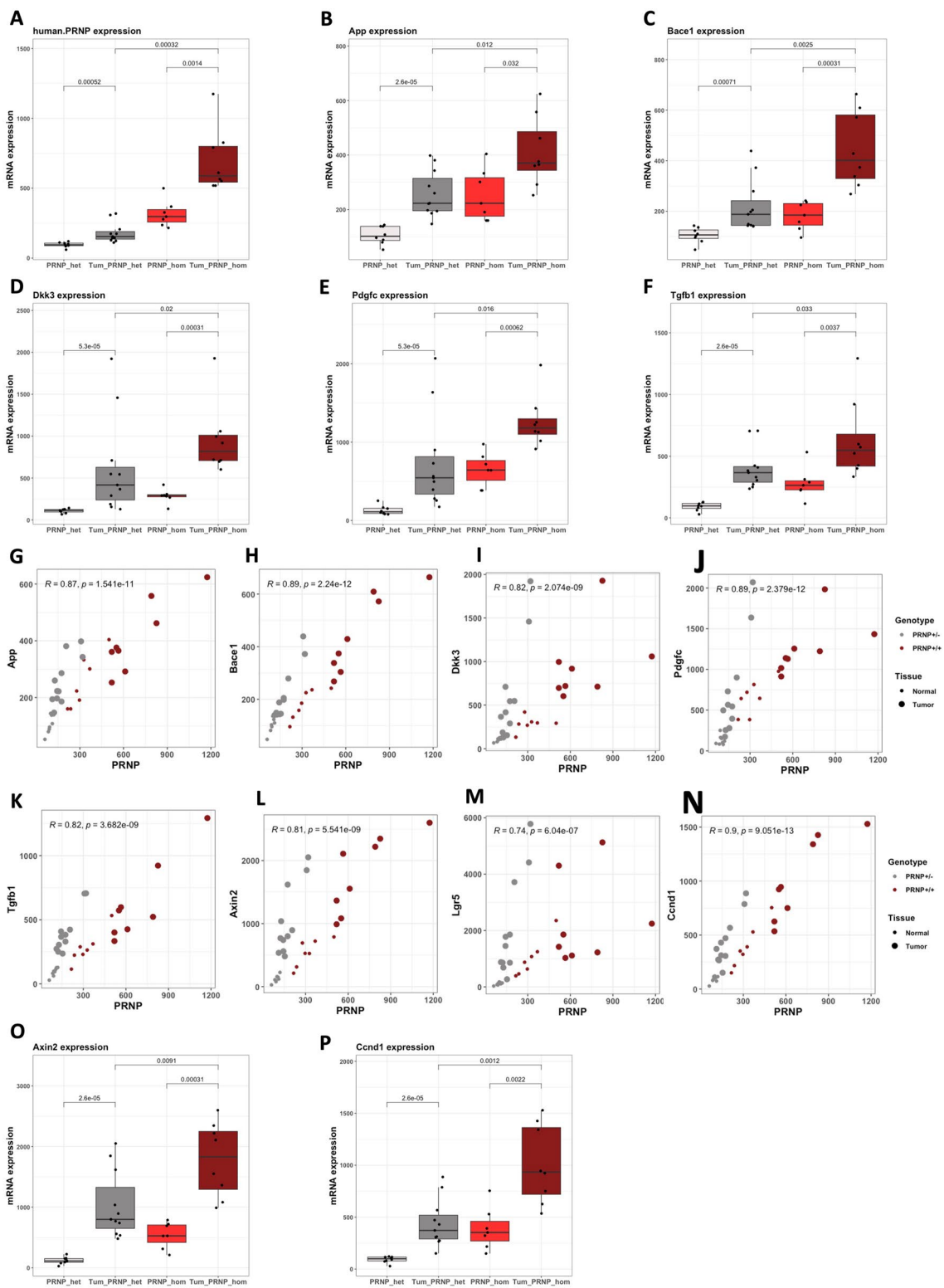


**Fig. 4** (See legend on previous page.)

normal tissue of both types of mice, and that the tumor levels were higher in homozygous versus heterozygous mice (Fig. 4B–F). We actually found that the expression levels of these genes were highly correlated to those of *PRNP* (Fig. 4G–K). In our mouse model, we further found that the levels of the Wnt target genes *Axin2*, *Lgr5* and *Ccnd1* were also strongly correlated to those of *PRNP* (Fig. 4L–N). As a result, the mean levels of *Axin2* and *Ccnd1* were much higher in tumors from homozygous than heterozygous mice (1.7 fold and 2.3 fold for *Axin2* and *Ccnd1*, respectively, Fig. 4O, P). At histological examination, *VilCreER<sup>T2</sup>Apc<sup>fl/+</sup>-PRNP<sup>+/-</sup>* mice exhibited a small number of adenomas or in situ adenocarcinomas (Fig. 5A–C), while *VilCreER<sup>T2</sup>Apc<sup>fl/+</sup>-PRNP<sup>+/+</sup>* mice were found to harbor numerous high-grade adenomas, in situ and even infiltrating adenocarcinomas, (Fig. 5A and D–E) suggesting that the overexpression of PrP<sup>C</sup> promotes colon cancer aggressiveness. In agreement, *PRNP<sup>+/+</sup>* tumors exhibited intense nuclear or cytoplasmic  $\beta$ -catenin staining (Fig. 5E, lower panels) in contrast to *PRNP<sup>+/-</sup>* tumors that present a lower accumulation of  $\beta$ -catenin (Fig. 5C, lower panel).

#### PRNP expression is induced in mouse models of liver cancer with $\beta$ -catenin activation

To possibly extend our observations, we turned to liver cancer models, in which activation of  $\beta$ -catenin is one the most frequent mutational event [39]. We first exploited a mouse model based on Cre-Lox inactivation of *Apc* in hepatocytes (*Apc<sup>Δhep</sup>*) that recapitulates both hepatocellular carcinoma and hepatoblastoma with aberrant  $\beta$ -catenin activation [22, 40, 41]. In the pre-tumoral setting, analysis of our ChIPseq data [41] indicated that *Tcf7l2*-encoded TCF4 bound to the *Prnp* promoter in hepatocytes shortly after  $\beta$ -catenin activation, which was not observed when  $\beta$ -catenin was invalidated (Fig. 6A), thus confirming our earlier data that TCF4 regulates *Prnp* expression through direct binding to its promoter region. In line with this, ATACseq analysis revealed a time-dependent opening of chromatin at the *Prnp* promoter in GFP + *Apc<sup>Δhep</sup>*-sorted hepatocytes, accompanied by *Prnp* transcription, as inferred through RNAseq (Fig. 6B). In qPCR experiments, we confirmed the induction of *Prnp* gene expression in tumors from *Apc<sup>Δhep</sup>* mice (Fig. 6C),

which was not observed in  $\beta$ -catenin-independent liver tumors induced by diethylnitrosamine (DEN) (Additional file 1: Fig. S5A). Of note, there was a tendency towards higher levels of *Prnp* in undifferentiated tumors, which resemble hepatoblastoma and display an epithelial to mesenchymal transition signature [22], as opposed to differentiated tumors that are similar to human hepatocellular carcinoma from G5–G6 groups (Fig. 6D). Similar results were obtained using RNAseq data from our previous study [22], combining liver tumors from either mutant *Cttnb1* deleted of exon 3 obtained by in vivo CRISPR/Cas9 editing or *Apc<sup>Δhep</sup>* mice (Fig. 6E). Interestingly, *Nr3c1* transcripts followed the same pattern of expression as *Prnp* (Fig. 6F), further reinforcing the link between PrP<sup>C</sup> and glucocorticoid signaling found in the context of colon cancer (see above), and the two Wnt target genes *Axin2* and *Ccnd1* were higher in undifferentiated as compared to differentiated tumors (Additional file 1: Fig. S5C, D). Finally, in the same dataset, we found that *Prnp* mRNA levels were significantly correlated to those of *App*, *Dkk3*, *Pdgfc*, *Tgfb1*, *Axin2*, *Ccnd1* and *Nr3c1* (Fig. 6G–M). Altogether, these results provide further evidence that *Prnp* is a target of the Wnt- $\beta$ -catenin pathway in multiple tissues and that it defines a signaling axis that is conserved from colon to liver cancer in mice.

#### The PRNP-CTNNB1-NR3C1 axis defines a group of CRC patients with dismal prognosis

From the above data, we may hypothesize that, in CRC patients,  $\beta$ -catenin and glucocorticoid pathway activation cooperatively induce *PRNP* expression and may, as a consequence, instigate a detrimental vicious circle. Accordingly and in line with our previous findings [9, 10] and those illustrated in Fig. 2G and 3G, *PRNP*, *BACE1*, *DKK3*, *PDGFC*, *NR3C1* and *TSC22D3* levels were all enriched in the CMS4 subgroups of tumors from the IDEA France cohort (Fig. S6A–F), uniquely composed of stage III CRC cases [24]. However, this was not the case for the canonical Wnt targets *AXIN2* and *LGR5* (Additional file 1: Fig. S6G, H), in line with data reported in cell lines [42]. In addition, the expression levels of *BACE1*, *DKK3*, *PDGFC*, *NR3C1* and *TSC22D3* were all significantly correlated with those of *PRNP* (Additional file 1: Fig. S6I–M). Finally, we found that genes from this network were all

(See figure on next page.)

**Fig. 5** PrP<sup>C</sup> overexpression aggravates the development of mutant *Apc* driven CRC in mouse. **A** Relative quantification of lesion types according to genotype. **B, C** H&E staining sections from *PRNP<sup>+/-</sup>* mice, showing representative zones of high grade dysplasia (**B**, bottom panel) and low grade dysplasia (**C**, middle panel), as well as  $\beta$ -catenin staining (**C**, bottom panel). **D, E** H&E staining sections from *PRNP<sup>+/+</sup>* mice, showing representative zones of infiltrating adenocarcinoma (**D**, bottom panels) and high grade dysplasia (**E**, middle panels), as well as  $\beta$ -catenin staining (**E**, bottom panels). Arrows indicate: a transition zone between normal cells and high grade dysplasia cells (**B**, bottom panel), mitoses (**E**, middle right panel), nuclear  $\beta$ -catenin (**E**, bottom right panel). Mice experiments were conducted as described in Additional file 1

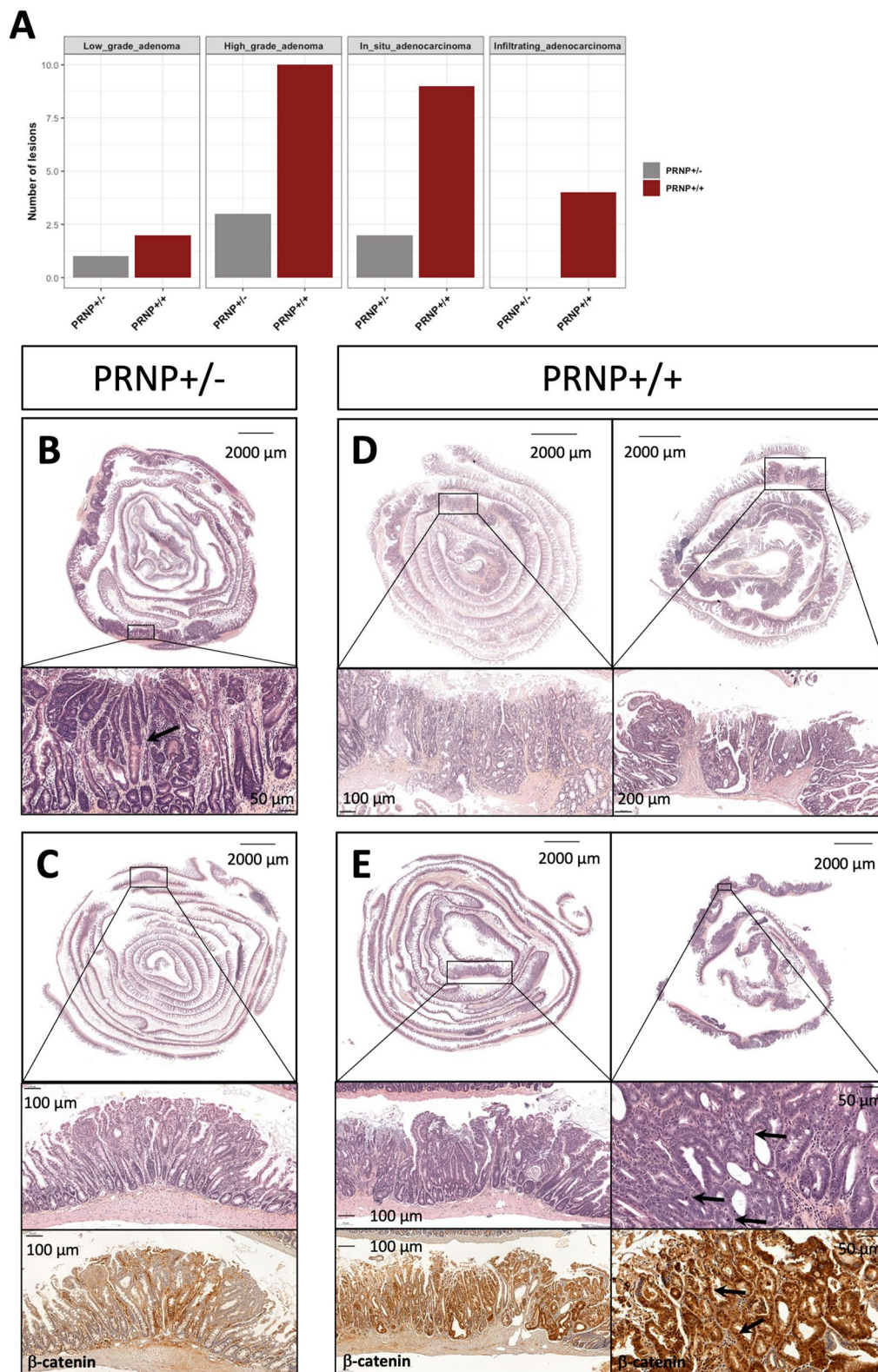


**Fig. 5** (See legend on previous page.)

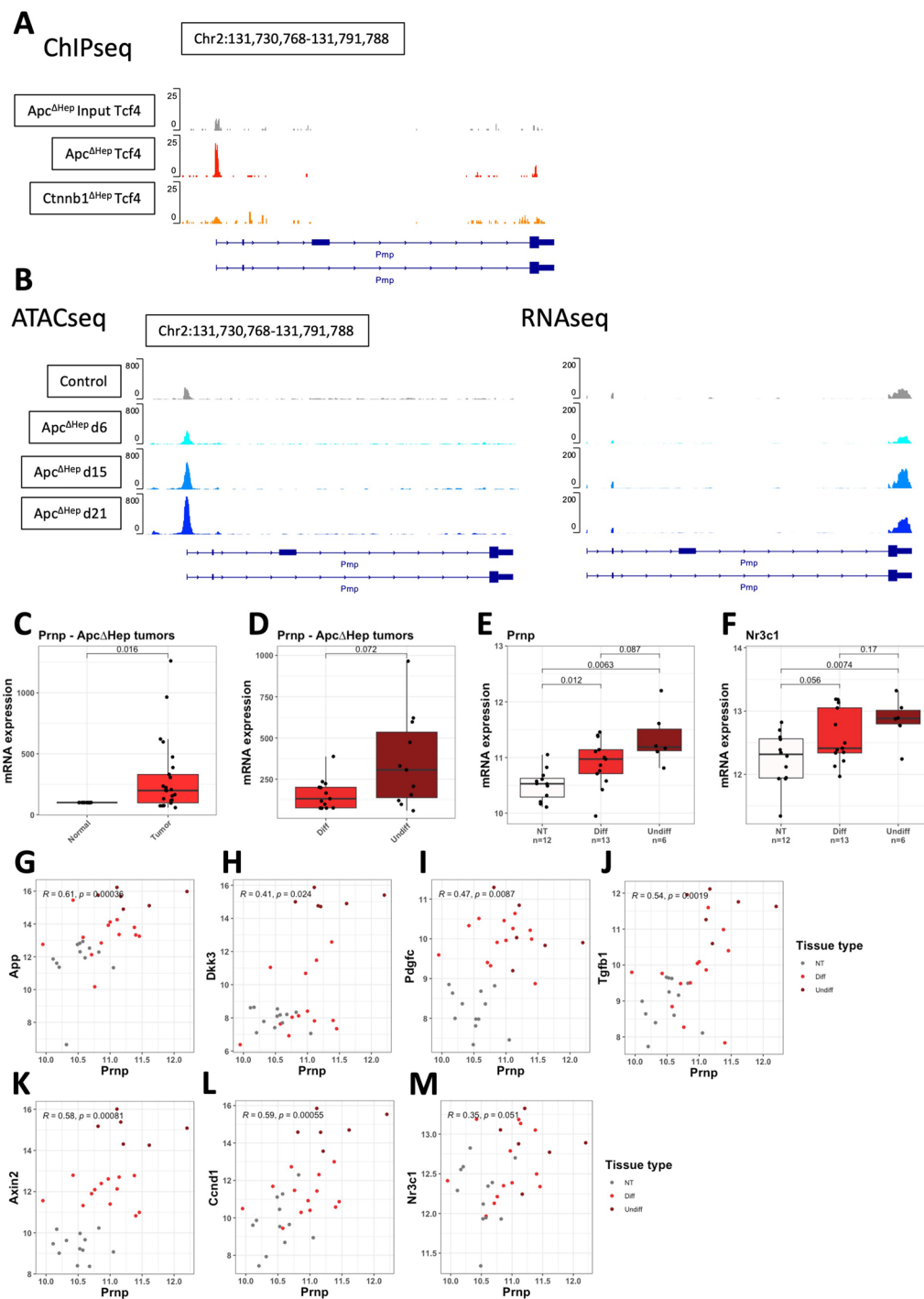


**Fig. 6** The *Prnp* gene is a target of Wnt- $\beta$ -catenin signaling in mouse models of liver cancer. **A** Analysis of our GSE35213 ChIPseq dataset reveals enrichment of the Tcf712-encoded TCF4 transcription factor at the promoter of the *Prnp* gene in *Apc*-inactivated (*Apc* $^{\Delta\text{hep}}$ ), but not control or *Ctnnb1*-deficient hepatocytes. **B** Analysis of our GSE242267 ATACseq dataset and our GSE210482 RNAseq showing the promoter accessibility (left) and RNA transcription (right) of the *Prnp* gene along the kinetics (days 6, 15 and 21) of *Apc* inactivation in hepatocytes as compared to GFP $^{\text{+}}$  control. **C** Boxplots showing the mRNA levels of *Prnp* in *Apc* $^{\Delta\text{hep}}$  tumor versus *Apc* $^{\Delta\text{hep}}$  normal tissue, as measured through qRT-PCR. **D** Boxplots showing the mRNA levels of *Prnp* in undifferentiated versus differentiated liver tumors from *Apc* $^{\Delta\text{hep}}$  mice, as measured through qRT-PCR. **E, F** Analysis of our PRJEB44400 dataset reveals increased *Prnp* (**E**) and *Nr3c1* (**F**) expression in differentiated and mostly undifferentiated liver tumors from mutant *Ctnnb1* and *Apc* mice. **G–M** Scatter plots showing the correlation between *Prnp* and *App* (**G**), *Dkk3* (**H**), *Pdgfr* (**I**), *Tgfb1* (**J**), *Axin2* (**K**), *Ccnd1* (**L**) and *Nr3c1* (**M**) mRNA levels in the PRJEB44400 dataset

enriched in the CMS combinations that we identified as associated with a notable dismal prognosis in our recent work [5] (Additional file 1: Fig. S6N–S). Again, opposite results were obtained for the two canonical Wnt targets *AXIN2* and *LGR5* (Additional file 1: Fig. S6T–U). Similar analyses in the PETACC8 cohort [26] yielded comparable results (Additional file 1: Fig. S7), although the correlations between *PRNP* and *BACE1* or *PDGFC* were modest as compared to those between *PRNP* and *DKK3*, *NR3C1* and *TSC22D3*, whose expression is majorly controlled by the GR (data not shown). The differences between the two cohorts may be accounted for by the different material used for 3'RNAseq (punch biopsies for the IDEA cohort and macro-dissected tissue sections for the PETACC8 cohort). Next, we calculated a *PRNP-CTNNB1-NR3C1* score and we found this score to be significantly higher in CMS4 patients from the IDEA France cohort (Fig. 7A). This score was also increased in the group of patients with a pejorative CMS combination (Fig. 7B) or in patients with high-risk disease (pT4 and/or N2) (Fig. 7C). Furthermore, major correlations were observed between the *PRNP-CTNNB1-NR3C1* score and a mesenchymal score derived from the study by de Reyniès et al. [43] (Fig. 7D), or a fibroblast score based on the MCP counter deconvolution algorithm [44] (Fig. 7E). As shown in Fig. 7F, the correlation between the mesenchymal and the *PRNP-CTNNB1-NR3C1* score featured among the highest in the IDEA-France cohort, arguing that the PrP<sup>C</sup>-Wnt-GR axis is a genuine hallmark of mesenchymal CRC.

A higher *PRNP-CTNNB1-NR3C1* score was also found in PETACC8 patients belonging to the CMS4 or the dismal prognosis CMS combination subgroups (Additional file 1: Fig. S8A, B). When we dichotomized patients from the IDEA France cohort according to this *PRNP-CTNNB1-NR3C1* score, we observed that patients with a high score segregated into the CMS4 subgroup (Fig. 7G and Additional file 1: Table S3) and were significantly associated with the poor CMS combination or high TNM risk subgroups (Additional file 1: Table S3). Patients with a high *PRNP-CTNNB1-NR3C1* score in the PETACC8 cohort were also more represented in the CMS4 and pejorative CMS combination groups (Additional file 1:

Fig. S8D). Finally, a high *PRNP-CTNNB1-NR3C1* score in the IDEA France cohort was associated with a significantly shorter time to recurrence than a low score (HR=1.44, CI=1.16–1.79,  $p < 0.001$ ) (Fig. 7H), which was even more apparent within the group of patients who received chemotherapy for 3 months instead of 6 months (HR=1.70, CI=1.26–2.29,  $p < 0.001$ ) (Fig. 7I). This was also true when considering only patients having been treated with FOLFOX (Additional file 1: Fig. S9A). Of note, the prognostic value of the 3 gene-combination was superior to those obtained when combining two out of three genes (Additional file 1: Fig. S9B–D). A higher *PRNP-CTNNB1-NR3C1* score was also associated with a worse prognosis in the entire PETACC8 cohort (HR=1.23, CI=1.01–1.50,  $p = 0.04$ ) (Additional file 1: Fig. S8E) or within each arm (Additional file 1: Fig. S8F, G). Altogether, these results exemplify the *PRNP-CTNNB1-NR3C1* axis as a poor prognosis trait of CRC.

## Discussion

This study uncovers a new gene regulatory network involving PrP<sup>C</sup>, the Wnt and Glucocorticoid signaling pathways that pertains to CRC progression and dismal outcome (Fig. 8) We have recently documented that PrP<sup>C</sup> is overexpressed in the mesenchymal, poor-prognosis subtype of CRC, and have shed some mechanistic insight into how it contributes to the mesenchymal phenotype of CRC cells [9, 32]. Going one step further, we have provided the proof of concept that antibody-mediated neutralization of PrP<sup>C</sup> may represent a novel therapeutic strategy to target mesenchymal CRC [10]. However, an integrated view of the mechanisms leading to the upregulation of PrP<sup>C</sup> was lacking. Several cancer studies have documented an induction of PrP<sup>C</sup> expression upon ER stress [45], hypoxia [46] or DNA damage [47]. From a molecular point of view, the *PRNP* promoter has been shown to be positively regulated by several transcription factors including sXBP1 [45], AP1 [48] as well as NFIL3 [49]. Here, we first uncovered that PrP<sup>C</sup> is a downstream target of the canonical Wnt- $\beta$ -catenin pathway through in silico and molecular analyses in several models of colon and liver cancer based on  $\beta$ -catenin overactivation. One major finding is that, in human, *PRNP* gene regulation

(See figure on next page.)

**Fig. 7** The *PRNP*-dependent axis is over-represented in poor-prognosis subtypes of CRC in the IDEA-France randomized clinical trial and predicts dismal outcome. **A–C** Relative *PRNP-CTNNB1-NR3C1* score according to the CMS classification (**A**), CMS combination (**B**) or TNM risk (**C**) in the IDEA France cohort. Patients with stage pT1–T3 and pN1 were classified as low TNM risk and those with pT4 and / or pN2 as high TNM risk. **D–F** Scatter plots showing the correlation between the *PRNP-CTNNB1-NR3C1* score and the mesenchymal (**D**) or the fibroblast (**E**) scores in the IDEA France cohort. **F** Density plot showing the distribution of correlation coefficients with the *PRNP-CTNNB1-NR3C1* score in the IDEA France cohort highlighting the top-ranked correlation with the mesenchymal score. **G** Sankey plots showing the correspondence between low or high *PRNP-CTNNB1-NR3C1* score and CMS subclasses. **H, I** Kaplan–Meier curves comparing time to recurrence in patients with low or high *PRNP-CTNNB1-NR3C1* score in the entire IDEA France cohort (**H**) or in the subset of patients having received chemotherapy during 3 months (**I**)

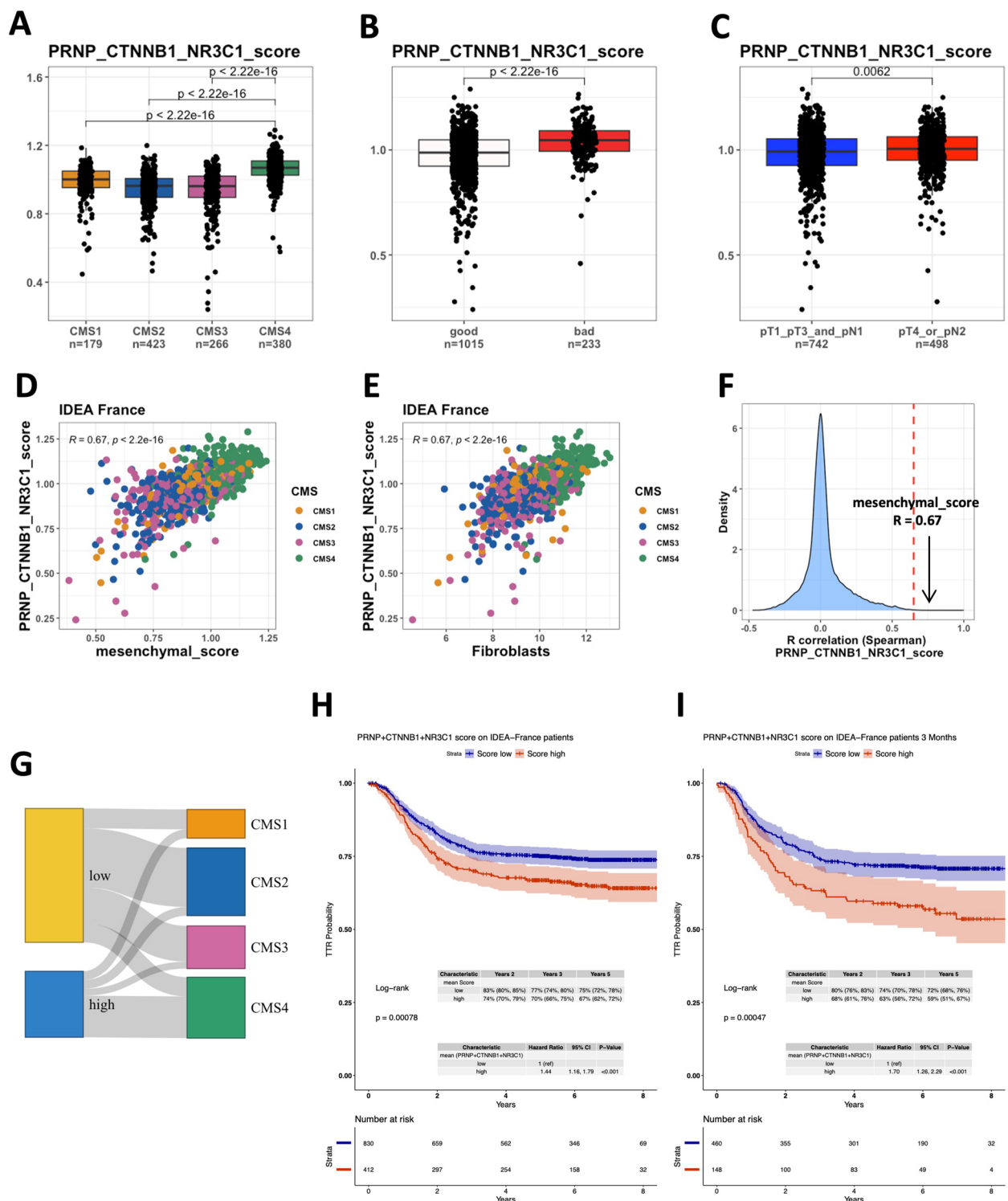


**Fig. 7** (See legend on previous page.)

is also highly modulated by glucocorticoid signaling. This observation fully fits in with the notion that the transcriptional response to Wnt- $\beta$ -catenin signaling is

highly context- and co-factor-dependent [30], and with the recent report that  $\beta$ -catenin partners with the GR to promote stemness properties of prostate cancer cells

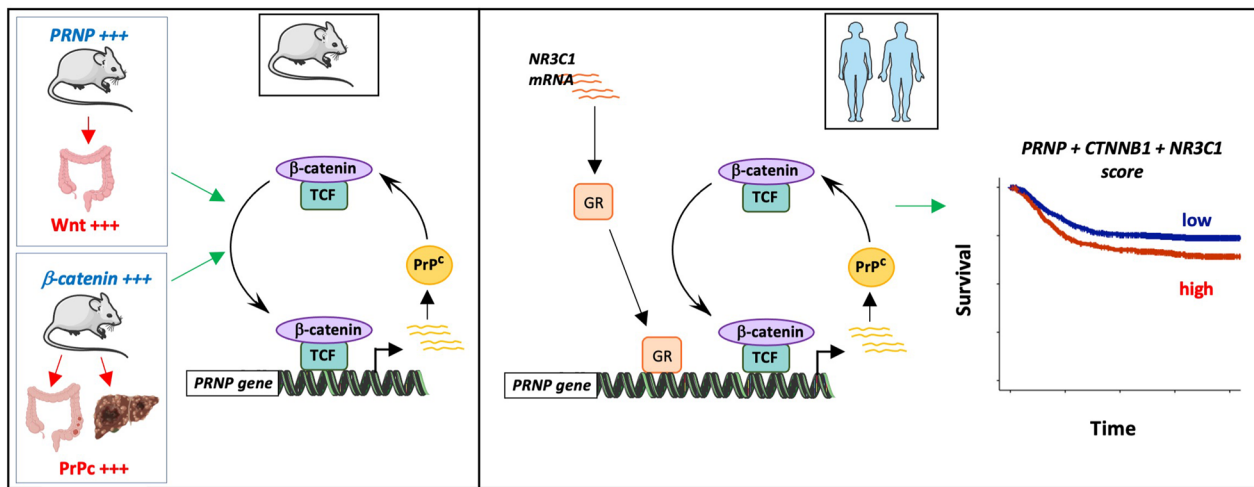


**Fig. 8** Graphical summary

[50]. That PrP<sup>C</sup> levels are sensitive to corticoids has been previously documented in neutrophils by Mariante et al. [51], but, to our knowledge, this is the first report that this also holds true in the context of cancer. Our results also align well with the current view that the specificity of gene expression regulation is highly dependent upon TF combinations [52]. In this respect, we may envision that additional regulatory factors beyond β-catenin and the GR combine with those to regulate *PRNP* gene expression. Potential candidates include SMADs, since they both interact with β-catenin [8] and the GR [53] and relay the action of TGFβ, itself known to induce the expression of PrP<sup>C</sup> [9, 51]. Further exploration is required to obtain an integrated view of the complex regulation of the *PRNP* gene in cancer.

While the study from Mariante and colleagues was performed in mice, our results obtained in human cohorts and mouse models, combined with comparative genomics of the regulatory sequences in the *PRNP* promoter, suggest that some aspects of *PRNP* regulation are specific to human, as reported for its regulation by the FOXP2 transcription factor [54]. This finding is reminiscent of the divergence of the p53 gene regulatory network between mouse and human emphasized by Fischer [55]. Incidentally, the identification of apparent inconsistencies after interrogating mouse and human datasets has sparked our search for potential β-catenin co-factors and led us to focus on the GR, whose response element differs between the mouse *Prnp* and human *PRNP* promoters. Besides, regardless of the differences between mouse and human, our generation of a *PRNP*-overexpressing *Apc* mouse model has proven instrumental to uncover the occurrence of a vicious circle deriving from the positive feedback loop linking PrP<sup>C</sup> to the Wnt signaling

pathway. Thus, despite limitations inherent to mouse studies, molecular and histological examination of our autochthonous mouse model has successfully informed us on the deleterious impact of the cooperation between PrP<sup>C</sup> and aberrant Wnt signaling. Such observations were made possible by the unique characteristics of our model of PrP<sup>C</sup> overexpression, insuring proper regulation of expression and gain of function. Of note, *Tgfb1* features among the genes that are induced downstream from PrP<sup>C</sup> (see Fig. 4F, K), suggesting that TGFβ1 may also fuel the vicious circle fostering *PRNP* gene expression, since we [9] and others [51] have documented a positive regulation of *PRNP* by TGFβ1.

Adding yet another layer of complexity, it is now recognized that the action of the GR can differ according to whether it is liganded or not [56]. This prompted us to include the GR target gene *TSC22D3* in our analyses, as a readout of GR activation. Given the reciprocal relations between stress and cancer [57, 58], an endogenous activation of the GR in CRC patients is very likely. Incidentally, we obtained prominent correlations between the expression of *TSC22D3* and that of *PRNP* (see Additional file 1: Fig. S6M) or the *PRNP-CTNNB1-NR3C1* score ( $R=0.55$ , Spearman) in the IDEA France cohort, indicating that tumors with high PrP<sup>C</sup> expression exhibit intrinsic GR activation. Furthermore, beyond the circulation, one source of glucocorticoids may be the tumor itself, as emphasized recently [59]. A major finding in the later study is that tumor-derived glucocorticoids exert a paracrine action on Tregs and foster tumor growth through Treg activation [59]. It can thus be surmised that the mobilization of the *PRNP-CTNNB1-NR3C1* axis in tumor cells is associated with the emergence of an immune-suppressive

tumor microenvironment. Another potential deleterious trait connected to the *PRNP-CTNNB1-NR3C1* axis would be the interference with therapy-induced anti-tumor immunity, as the induction of *TSC22D3* in dendritic cells (DCs) by glucocorticoids was shown to block interferon responses and subsequent T cell activation [60]. Altogether, these different processes may account for the dismal prognosis exemplified in patients with a high *PRNP-CTNNB1-NR3C1* score.

Importantly, we obtained a set of observations that consistently conspire to define high *PRNP-CTNNB1-NR3C1* as a pejorative trait in CRC, in addition to its prognostic value. Indeed, we found the *PRNP-CTNNB1-NR3C1* score to be higher in CRC tumors of the CMS4 subtype, those with a pejorative CMS combination, or those associated with a higher risk of relapse based on TNM staging. One key finding is the very robust correlation between the *PRNP-CTNNB1-NR3C1* score and the mesenchymal score defined by [43], arguing that the *PRNP-CTNNB1-NR3C1* axis may be a hallmark of mesenchymal tumors.

## Conclusion

In summary, the integration of in silico, cellular, mouse and human data allowed us to uncover an unprecedented cooperation between Wnt, GR and PrP<sup>C</sup> signaling, which perpetuates a vicious circle in CRC. We found that the regulation of PrP<sup>C</sup> expression is not strictly transposable from mouse to human, but that the manipulation of PrP<sup>C</sup> expression in mouse can nonetheless help uncover regulatory networks, which subsequently proved to have clinical value. Our work thus advocates for the implementation of multimodal approaches to decipher the complexity of CRC. Finally, given the premises of PrP<sup>C</sup> targeting [10], this study may pave the way towards new therapeutic strategies to treat mesenchymal CRC.

## Abbreviations

APP	Amyloid precursor protein
CMS	Consensus molecular subtype
CRC	Colorectal cancer
DEN	Dimethylnitrosamine
Dex	Dexamethasone
GR	Glucocorticoid receptor
GRE	GR responsive element
HR	Hazard ratio
ILK	Integrin linked kinase
OPC	Oligodendrocyte progenitor cell
PrP <sup>C</sup>	Cellular prion protein
TF	Transcription factor
WRE	Wnt-responsive element

## Supplementary Information

The online version contains supplementary material available at <https://doi.org/10.1186/s12967-024-05164-0>.

**Additional file 1.** Materials and methods.

## Acknowledgements

The authors wish to thank the technical assistance of animal facilities staff at INRAE and Centre de Recherche des Cordeliers.

## Author contributions

SMR Conceived and supervised the study, performed molecular and bioinformatic analyses, wrote the manuscript. AG Performed animal studies, analyzed and interpreted animal experimental and in silico data. BP Performed animal studies. CB Analyzed and interpreted animal experimental. DLC, CJ and FD Participated in molecular and cellular biology experiments. CLP, JL and MV Participated in histological experiments. JC and NDC Participated in animal studies. MS, CJ, CP and AdR Contributed to assembling patient cohort RNAseq data. SC, JLV, BR Provided animal resources and funding. TA and JT Assembled patient cohorts. PLP Contributed to design the study, assembled patient cohorts, analyzed patient data, provided funding and reviewed the manuscript. All authors read and approved the manuscript.

## Funding

This work was supported by INSERM, INRAE, as well as Cancéropôle Ile de France (grant number 2016-1-EMERG-36-UP 5-1), Association pour la Recherche sur le Cancer (grant number PJA 20171206220), SIRIC CARPEM (CAncer Research for PErsonalized Medicine, INCa-DGOS Inserm\_12561), Labex Immuno-oncology, Groupement des Entreprises Monégasques dans la Lutte contre le Cancer (GEMLUC), Plan cancer (grant CHROMALIV), Agence Nationale de la Recherche (JCJC DLK1-EPLIV) and the Ligue Nationale Contre le Cancer (Team labellisation for SC, BR and PLP). MS was supported by a fellowship from Fondation pour la Recherche Médicale (FRM grant FDM202006011237) and CJ by a PhD fellowship from the Ligue Nationale Contre le Cancer.

## Data availability

Materials, data, and protocols described in the manuscript will be made available upon reasonable request.

## Declarations

## Competing interests

The authors declare no competing interests in the present study.

## Author details

<sup>1</sup>Centre de Recherche Des Cordeliers, INSERM, Sorbonne Université, Université Paris Cité, 75006 Paris, France. <sup>2</sup>University of Paris-Saclay, INRAE, AgroParis-Tech, UMR1313 GABI, 78350 Jouy-en-Josas, France. <sup>3</sup>Institut du Cancer Paris CARPEM, APHP, Department of Pathology, APHP-Centre-Université Paris Cité, Hôpital Européen G. Pompidou, Paris, France. <sup>4</sup>Université Paris Cité, Institut Cochin, Inserm, CNRS, F-75014 Paris, France. <sup>5</sup>Equipe Labellisée Ligue Nationale Contre Le Cancer, Paris, France. <sup>6</sup>Institut du Cancer Paris CARPEM, APHP, Hepatogastroenterology and GI Oncology Department, APHP-Centre-Université Paris Cité, Hôpital Européen G. Pompidou, Paris, France. <sup>7</sup>Histology, Imaging and Cytometry Center (CHIC), Paris, France. <sup>8</sup>Saint-Antoine Hospital, INSERM, Unité Mixte de Recherche Scientifique 938, Sorbonne Université, Paris, France. <sup>9</sup>Institut du Cancer Paris CARPEM, APHP, Department of Biology, APHP-Centre-Université Paris Cité, Hôpital Européen G. Pompidou, Paris, France.

Received: 12 February 2024 Accepted: 4 April 2024

Published online: 08 April 2024

## References

1. Sung H, Ferlay J, Siegel RL, Laversanne M, Soerjomataram I, Jemal A, et al. Global Cancer Statistics 2020: GLOBOCAN estimates of incidence and mortality worldwide for 36 cancers in 185 countries. *CA Cancer J Clin*. 2021;71:209–49.



2. Kinzler KW, Nilbert MC, Su LK, Vogelstein B, Bryan TM, Levy DB, et al. Identification of FAP locus genes from chromosome 5q21. *Science*. 1991;253:661–5.
3. Parsons MJ, Tammela T, Dow LE. WNT as a driver and dependency in cancer. *Cancer Discov*. 2021;11:2413–29.
4. Guinney J, Dienstmann R, Wang X, de Reyniès A, Schlicker A, Sonesson C, et al. The consensus molecular subtypes of colorectal cancer. *Nat Med*. 2015;21:1350–6.
5. Marisa L, Blum Y, Taieb J, Ayadi M, Pilati C, Le Malicot K, et al. Intratumor CMS heterogeneity impacts patient prognosis in localized colon cancer. *Clin Cancer Res*. 2021;27:4768–80.
6. Tauriello DVF, Sancho E, Batlle E. Overcoming TGF $\beta$ -mediated immune evasion in cancer. *Nat Rev Cancer*. 2022;22:25–44.
7. Mouillet-Richard S, Laurent-Puig P. YAP/TAZ signalling in colorectal cancer: lessons from consensus molecular subtypes. *Cancers*. 2020;12:3160.
8. Qin K, Yu M, Fan J, Wang H, Zhao P, Zhao G, et al. Canonical and non-canonical Wnt signaling: multilayered mediators, signaling mechanisms and major signaling crosstalk. *Genes Dis*. 2024;11:103–34.
9. Le Corre D, Ghazi A, Balogoun R, Pilati C, Aparicio T, Martin-Lannerée S, et al. The cellular prion protein controls the mesenchymal-like molecular subtype and predicts disease outcome in colorectal cancer. *EBioMedicine*. 2019;46:94–104.
10. Mouillet-Richard S, Martin-Lannerée S, Le Corre D, Hirsch TZ, Ghazi A, Sroussi M, et al. A proof of concept for targeting the PrPC - Amyloid  $\beta$  peptide interaction in basal prostate cancer and mesenchymal colon cancer. *Oncogene*. 2022;41:4397–404.
11. Mouillet-Richard S, Ghazi A, Laurent-Puig P. The cellular prion protein and the hallmarks of cancer. *Cancers*. 2021;13:5032.
12. Hirsch TZ, Martin-Lannerée S, Mouillet-Richard S. Functions of the prion protein. *Prog Mol Biol Transl Sci*. 2017;150:1–34.
13. Mouillet-Richard S, Ermonval M, Chebassier C, Laplanche JL, Lehmann S, Launay JM, et al. Signal transduction through prion protein. *Science*. 2000;289:1925–8.
14. Lee R, Li J, Li J, Wu C-J, Jiang S, Hsu W-H, et al. Synthetic essentiality of tryptophan 2,3-dioxygenase 2 in APC-mutated colorectal cancer. *Cancer Discov*. 2022;12:1702–17.
15. Marei H, Tsai W-TK, Kee Y-S, Ruiz K, He J, Cox C, et al. Antibody targeting of E3 ubiquitin ligases for receptor degradation. *Nature*. 2022;610:182–9.
16. Flanagan DJ, Pentimikko N, Luopajarvi K, Willis NJ, Gilroy K, Raven AP, et al. NOTUM from Apc-mutant cells biases clonal competition to initiate cancer. *Nature*. 2021;594:430–5.
17. Skrzypczak M, Goryca K, Rubel T, Paziewska A, Mikula M, Jarosz D, et al. Modeling oncogenic signaling in colon tumors by multidirectional analyses of microarray data directed for maximization of analytical reliability. *PLoS ONE*. 2010;5: e13091.
18. Sabates-Bellver J, Van der Flier LG, de Palo M, Cattaneo E, Maake C, Rehrauer H, et al. Transcriptome profile of human colorectal adenomas. *Mol Cancer Res*. 2007;5:1263–75.
19. Galamb O, Györfy B, Sipos F, Spisák S, Németh AM, Miheller P, et al. Inflammation, adenoma and cancer: objective classification of colon biopsy specimens with gene expression signature. *Dis Markers*. 2008;25:1–16.
20. Marisa L, de Reyniès A, Duval A, Selves J, Gaub MP, Vescovo L, et al. Gene expression classification of colon cancer into molecular subtypes: characterization, validation, and prognostic value. *PLoS Med*. 2013;10: e1001453.
21. Gobert RP, Joubert L, Curchod M-L, Salvat C, Foucault I, Jorand-Lebrun C, et al. Convergent functional genomics of oligodendrocyte differentiation identifies multiple autoinhibitory signaling circuits. *Mol Cell Biol*. 2009;29:1538–53.
22. Loesch R, Caruso S, Paradis V, Godard C, Gougelet A, Renault G, et al. Deleting the  $\beta$ -catenin degradation domain in mouse hepatocytes drives hepatocellular carcinoma or hepatoblastoma-like tumor growth. *J Hepatol*. 2022;77:424–35.
23. Sanceau J, Poupel L, Joubel C, Lagoutte I, Caruso S, Pinto S, et al. DLK1/DIO3 locus upregulation by a  $\beta$ -catenin-dependent enhancer drives cell proliferation and liver tumorigenesis. *Mol Ther*. 2024;51525–0016(24):00037–46.
24. André T, Vernerey D, Mineur L, Bennouna J, Desrame J, Faroux R, et al. Three versus 6 months of oxaliplatin-based adjuvant chemotherapy for patients with stage III colon cancer: disease-free survival results from a randomized, open-label, international duration evaluation of adjuvant (IDEA) France, Phase III. *Trial J Clin Oncol*. 2018;36:1469–77.
25. Gallois C, Sroussi M, Andre T, Mouillet-Richard S, Agueeff N, Vernerey D, et al. Predictive models of recurrence from transcriptomic signatures of the tumor microenvironment and cell cycle in stage III colon cancer from PETACC-8 and IDEA France trials. *J Clin Oncol*. 2023;41:3523.
26. Taieb J, Tabernero J, Mini E, Subtil F, Folprecht G, Van Laethem J-L, et al. Adjuvant FOLFOX4 +/- Cetuximab in KRAS wild-type patients with resected stage III colon cancer results from the PETACC8 intergroup trial. *Ann Oncol*. 2012;23:17–17.
27. Wan C, Mahara S, Sun C, Doan A, Chua HK, Xu D, et al. Genome-scale CRISPR-Cas9 screen of Wnt/ $\beta$ -catenin signaling identifies therapeutic targets for colorectal cancer. *Sci Adv*. 2021;7:eabf2567.
28. Sandelin A, Alkema W, Engström P, Wasserman WW, Lenhard B. JASPAR: an open-access database for eukaryotic transcription factor binding profiles. *Nucleic Acids Res*. 2004;32:D91–4.
29. de Wit M, Jimenez CR, Carvalho B, Belien JAM, Delis-van Diemen PM, Mongera S, et al. Cell surface proteomics identifies glucose transporter type 1 and prion protein as candidate biomarkers for colorectal adenoma-to-carcinoma progression. *Gut*. 2012;61:855–64.
30. Nakamura Y, de Paiva AE, Veenstra GJC, Hoppler S. Tissue- and stage-specific Wnt target gene expression is controlled subsequent to  $\beta$ -catenin recruitment to cis-regulatory modules. *Development*. 2016;143:1914–25.
31. Alanis-Lobato G, Andrade-Navarro MA, Schaefer MH. HIPPIE v2.0: enhancing meaningfulness and reliability of protein-protein interaction networks. *Nucleic Acids Res*. 2017;45:D408–14.
32. Ghazi A, Le Corre D, Pilati C, Taieb J, Aparicio T, Didelot A, et al. Prognostic value of the PrPC-ILK-IDO1 axis in the mesenchymal colorectal cancer subtype. *Oncoimmunology*. 2021;10:1940674.
33. Besnier LS, Cardot P, Da Rocha B, Simon A, Loew D, Klein C, et al. The cellular prion protein PrPc is a partner of the Wnt pathway in intestinal epithelial cells. *Mol Biol Cell*. 2015;26:3313–28.
34. Colnot S, Niwa-Kawakita M, Hamard G, Godard C, Le Plenier S, Houbron C, et al. Colorectal cancers in a new mouse model of familial adenomatous polyposis: influence of genetic and environmental modifiers. *Lab Invest*. 2004;84:1619–30.
35. el Marjou F, Janssen K-P, Chang BH-J, Li M, Hindie V, Chan L, et al. Tissue-specific and inducible Cre-mediated recombination in the gut epithelium. *Genesis*. 2004;39:186–93.
36. Lévy J, Cacheux W, Bara MA, L'Hermitte A, Lepage P, Fraudeau M, et al. Intestinal inhibition of Atg7 prevents tumour initiation through a microbiome-influenced immune response and suppresses tumour growth. *Nat Cell Biol*. 2015;17:1062–73.
37. Béringue V, Le Dur A, Tixador P, Reine F, Lepourry L, Perret-Liaudet A, et al. Prominent and persistent extraneural infection in human PrP transgenic mice infected with variant CJD. *PLoS ONE*. 2008;3: e1419.
38. Fischer M, Rulicke T, Raeber A, Sailer A, Moser M, Oesch B, et al. Prion protein (PrP) with amino-proximal deletions restoring susceptibility of PrP knockout mice to scrapie. *Embo J*. 1996;15:1255–64.
39. Laurent-Puig P, Zucman-Rossi J. Genetics of hepatocellular tumors. *Oncogene*. 2006;25:3778–86.
40. Colnot S, Decaens T, Niwa-Kawakita M, Godard C, Hamard G, Kahn A, et al. Liver-targeted disruption of Apc in mice activates beta-catenin signaling and leads to hepatocellular carcinomas. *Proc Natl Acad Sci U S A*. 2004;101:17216–21.
41. Gougelet A, Torre C, Veber P, Sartor C, Bachelot L, Denechaud P-D, et al. T-cell factor 4 and  $\beta$ -catenin chromatin occupancies pattern zonal liver metabolism in mice. *Hepatology*. 2014;59:2344–57.
42. Linnekamp JF, van Hooff SR, Prasetyanti PR, Kandimalla R, Buikhuisen JY, Fessler E, et al. Consensus molecular subtypes of colorectal cancer are recapitulated in vitro and in vivo models. *Cell Death Differ*. 2018;25:616–33.
43. de Reyniès A, Jaurand M-C, Renier A, Couchy G, Hysi I, Elarouci N, et al. Molecular classification of malignant pleural mesothelioma: identification of a poor prognosis subgroup linked to the epithelial-to-mesenchymal transition. *Clin Cancer Res*. 2014;20:1323–34.
44. Becht E, de Reyniès A, Giraldo NA, Pilati C, Buttard B, Lacroix L, et al. Immune and stromal classification of colorectal cancer is associated with molecular subtypes and relevant for precision immunotherapy. *Clin Cancer Res*. 2016;22:4057–66.

45. Dery MA, Jodoin J, Ursini-Siegel J, Aleynikova O, Ferrario C, Hassan S, et al. Endoplasmic reticulum stress induces PRNP prion protein gene expression in breast cancer. *Breast Cancer Res.* 2013;15:R22.
46. Park J-Y, Jeong J-K, Lee J-H, Moon J-H, Kim S-W, Lee Y-J, et al. Induction of cellular prion protein (PrP<sup>c</sup>) under hypoxia inhibits apoptosis caused by TRAIL treatment. *Oncotarget.* 2015;6:5342–53.
47. Bravard A, Auvré F, Fantini D, Bernardino-Sgherri J, Sissoëff L, Daynac M, et al. The prion protein is critical for DNA repair and cell survival after genotoxic stress. *Nucleic Acids Res.* 2015;43:904–16.
48. Bernardino-Sgherri J, Siberchicot C, Auvré F, Busso D, Brocas C, El Masri G, et al. Tumor resistance to radiotherapy is triggered by an ATM/TAK1-dependent-increased expression of the cellular prion protein. *Oncogene.* 2021;40:3460–9.
49. Lin S-C, Lin C-H, Shih N-C, Liu H-L, Wang W-C, Lin K-Y, et al. Cellular prion protein transcriptionally regulated by NFIL3 enhances lung cancer cell lamellipodium formation and migration through JNK signaling. *Oncogene.* 2020;39:385–98.
50. Martinez SR, Elix CC, Ochoa PT, Sanchez-Hernandez ES, Alkashgari HR, Ortiz-Hernandez GL, et al. Glucocorticoid receptor and  $\beta$ -catenin interact in prostate cancer cells and their co-inhibition attenuates tumorsphere formation, stemness, and docetaxel resistance. *Int J Mol Sci.* 2023;24:7130.
51. Mariante RM, Nobrega A, Martins RA, Areal RB, Bellio M, Linden R. Neuro-immunoendocrine regulation of the prion protein in neutrophils. *J Biol Chem.* 2012;287:35506–15.
52. Reiter F, Wienerroither S, Stark A. Combinatorial function of transcription factors and cofactors. *Curr Opin Genet Dev.* 2017;43:73–81.
53. Petta I, Dejager L, Ballegeer M, Lievens S, Tavernier J, De Bosscher K, et al. The interactome of the glucocorticoid receptor and its influence on the actions of glucocorticoids in combatting inflammatory and infectious diseases. *Microbiol Mol Biol Rev MMBR.* 2016;80:495–522.
54. Konopka G, Bomar JM, Winden K, Coppola G, Jonsson ZO, Gao F, et al. Human-specific transcriptional regulation of CNS development genes by FOXP2. *Nature.* 2009;462:213–7.
55. Fischer M. Conservation and divergence of the p53 gene regulatory network between mice and humans. *Oncogene.* 2019;38:4095–109.
56. Cirstea IC, Moll HP, Tuckermann J. Glucocorticoid receptor and RAS: an unexpected couple in cancer. *Trends Cell Biol.* 2023;33:594–604.
57. Eckerling A, Ricon-Becker I, Sorski L, Sandbank E, Ben-Eliyahu S. Stress and cancer: mechanisms, significance and future directions. *Nat Rev Cancer.* 2021;21:767–85.
58. Ma Y, Kroemer G. The cancer-immune dialogue in the context of stress. *Nat Rev Immunol.* 2023;24:264–81.
59. Taves MD, Otsuka S, Taylor MA, Donahue KM, Meyer TJ, Cam MC, et al. Tumors produce glucocorticoids by metabolite recycling, not synthesis, and activate Tregs to promote growth. *J Clin Invest.* 2023;133: e164599.
60. Yang H, Xia L, Chen J, Zhang S, Martin V, Li Q, et al. Stress-glucocorticoid-TSC22D3 axis compromises therapy-induced antitumor immunity. *Nat Med.* 2019;25:1428–41.

## Publisher's Note

Springer Nature remains neutral with regard to jurisdictional claims in published maps and institutional affiliations.